Pergamon

Geochimica et Cosmochimica Acta, Vol. 67, No. 14, pp. 2551–2560, 2003
Copyright © 2003 Elsevier Science Ltd
Printed in the USA. All rights reserved
0016-7037/03 $30.00 + .00

doi:10.1016/S0016-7037(03)00096-6

ATR-FTIR spectroscopic studies of boric acid adsorption on hydrous ferric oxide

DEREK PEAK,[1,*] GEORGE W. LUTHER, III,[2] and DONALD L. SPARKS[3]

[1]Department of Soil Science, University of Saskatchewan, Saskatoon, SK S7N 5A8, Canada
[2]College of Marine Studies, University of Delaware, Lewes, DE 19958, USA
[3]Department of Plant and Soil Sciences, University of Delaware, Newark, DE 19717, USA

(*Received August* 7, 2002; *accepted in revised form January* 30, 2003)

Abstract—Boron is an important micronutrient for plants, but high B levels in soils are often responsible for toxicity effects in plants. It is therefore important to understand reactions that may affect B availability in soils. In this study, Attenuated Total Reflectance Fourier transform Infrared (ATR-FTIR) spectroscopy was employed to investigate mechanisms of boric acid ($B(OH)_3$) and borate ($B(OH)_4^-$) adsorption on hydrous ferric oxide (HFO). On the HFO surface, boric acid adsorbs via both physical adsorption (outer-sphere) and ligand exchange (inner-sphere) reactions. Both trigonal (boric acid) and tetrahedral (borate) boron are complexed on the HFO surface, and a mechanism where trigonal boric acid in solution reacts to form either trigonal or tetrahedral surface complexes is proposed based upon the spectroscopic results. The presence of outer-sphere boric acid complexes can be explained based on the Lewis acidity of the B metal center, and this complex has important implications for boron transport and availability. Outer-sphere boric acid is more likely to leach downward in soils in response to water flow. Outer-sphere boron would also be expected to be more available for plant uptake than more strongly bound boron complexes, and may more readily return to the soil solution when solution concentrations decrease. *Copyright © 2003 Elsevier Science Ltd*

1. INTRODUCTION

Boric acid $B(OH)_3$ and its anion borate $B(OH)_4^-$ have solution chemistry that is quite different from most other oxyanions. Borate forms by the addition of a hydroxyl group to the trigonal planar boric acid molecule, forming a tetrahedral anion. The pK of this reaction is 9.2 (Shriver et al., 1994).

$$B(OH)_3 + OH^- \leftrightarrow B(OH)_4^- \qquad pKa = 9.2$$

Boric acid and borate both typically exist as monomers in solution at low concentrations (below 25 mM) but at higher concentrations many poly-borate polymers are known to form (Cotton and Wilkinson, 1980). Boron is an essential micronutrient for plant growth. Like many micronutrients, boron is required in low concentrations for the growth of plants but can be quite toxic to plants at higher levels. The range between these extremes is quite narrow. Borate toxicity is a major concern for agriculture in both arid regions of the United States and in poorly drained soils of high salinity. High levels of borate are also commonly found in irrigation water. Borate deficiency has also been reported in over 40 U.S. states (Keren and Bingham, 1985).

Most of the research of boron chemistry by soil chemists has provided information about the sorption of boron on soils and soil components. In all cases, researchers have noted that boron adsorption results in a bell-shaped pH envelope, with an adsorption maximum occurring near the pKa of boric acid (pH 9.2). Researchers have shown that the mineralogy of the sorbent has a large role on both the extent and mechanism of borate adsorption. Goldberg and colleagues (1993) found that ionic strength effects could be used to separate boron adsorption mechanisms on soil components and on soils. They used batch adsorption experiments and electrophoretic mobility experiments to study these ionic strength effects. On variably charged sorbents such as metal oxides and kaolinite, an inner-sphere complexation mechanism is suggested by the small influence of ionic strength on adsorption as well as by a shift of the point of zero charge to lower pH. A large ionic strength dependence was observed on montmorillonite and whole soils, suggesting an outer-sphere adsorption mechanism for boron. Electrophoretic mobility experiments on these permanently charged sorbents were not feasible, as they have a negative charge overall pH.

Interestingly (and somewhat counter-intuitively), boron adsorption at high ionic strength is sometimes greater than at low ionic strength. Research by Keren and coworkers examined this phenomenon in more detail (Keren and O'Conner, 1982, Keren and Sparks, 1994), and McBride (1997) later used some of this data to demonstrate shortcomings of diffuse layer models based on DLVO theory. By comparing the adsorption of boron on illite and montmorillonite (common 2:1 clay minerals) in CaCl and NaCl solutions of constant ionic strength (Keren and O'Connor, 1982), it was shown that Ca stimulated boron adsorption on montmorillonite far more than Na. This was explained by the fact that in alkaline conditions borate reaction with aluminol edge sites on 2:1 clay minerals is limited by the negative permanent charge of the planar sites of both montmorillonite and illite. At higher ionic strength (and in the presence of divalent cations) this surface charge is minimized by nonspecific adsorption of cations, the electrical double layer is compressed, and borate reaction with edge sites of the clay becomes more favorable. In the case of illite, much of the interlayer sites are filled with fixed potassium. This potassium satisfies much of the permanent charge of this clay mineral and as a result there is less effect of ionic strength on borate adsorption. The importance of sorbent mineralogy was also investigated by studying the adsorption of boron on pyrophyl-

* Author to whom correspondence should be addressed (derek.peak@usask.ca).

lite (Keren and Sparks, 1994). Since pyrophyllite is an ideal 2:1 clay mineral, it has no permanent charge due to isomorphic substitution and no interlayer space. This results in far less charge repulsion and therefore a greater boron adsorption capacity.

Few spectroscopic studies of boron interactions with soil components have been attempted. Beyrouty et al. (1984) used transmission mode FTIR spectroscopy to investigate the effect that boric acid adsorption had on the crystallization of an aluminum hydroxide gel. It was determined that boric acid adsorption retarded the transformation of amorphous aluminum hydroxide to gibbsite. The researchers concluded that due to this inhibition of gibbsite formation the boron must form direct bonds to the aluminum hydroxide. Potentiometric titrations also showed that the PZC of the gel was lowered in the presence of boric acid, suggesting specific adsorption. However, the researchers could not determine the exact nature of boron adsorption with FTIR and concluded that precipitation, adsorption, and surface polymerization were all possible. In a similar experiment, Su and Suarez (1997) used diffuse reflectance FTIR (DRIFT) to study boron sorption and release from allophane, an amorphous aluminosilicate. They compared the sorption of boric acid on allophane after mineral precipitation to the precipitation of allophane in the presence of boric acid. They determined that both trigonal and tetrahedral boron was present, with trigonal boric acid being the dominant sorbed species. More boron was sorbed when the allophane was coprecipitated with boric acid, and the resulting product had more tetrahedral boron (borate) than the samples where boron was sorbed to allophane after precipitation. It was assumed that borate could substitute for silicate in the allophane structure. It must be stressed that it is possible that sample preparation (dilution in KBr after sample drying or dilution of moist samples) could have affected the results of both these experiments.

Su and Suarez (1995) also used ATR-FTIR spectroscopy to study the adsorption of boric acid on soil components in situ. They examined boron adsorption on amorphous aluminum and iron oxides, allophane, kaolinite, quartz, and calcite over a range of pH and boron surface loadings. Unfortunately, interference of Si-O and Al-O infrared bands with tetrahedral boron peaks made a clear interpretation of the aluminum oxide, allophane, and quartz adsorption spectra impossible. In the iron hydroxide samples, they saw clear evidence of trigonal boron at pH 7, a mixture of both trigonal and tetrahedral boron at pH 9, and the spectra were dominated by tetrahedral boron at pH 11. The possibility of polymeric boron and boron precipitation was mentioned, but could not be distinguished from boron adsorption in their studies.

The objectives of this study were to examine complexation of boric acid and borate with hydrous ferric oxide (HFO) in situ over a range of pH (6.5–11.5) and at concentrations well below bulk polymerization of boron (50 μM-1 mM). Previous studies of HFO/boron interactions (Su and Suarez, 1995) found that trigonal and tetrahedral boron complexes form on HFO, but some of their spectra were collected at concentrations close to bulk polymerization (up to 23 mM B). If one is to utilize FTIR spectroscopy to accomplish these objectives, it is important to fully understand how infrared spectra of different boron compounds are affected by their molecular structure.

The majority of boron infrared studies concentrate on distinguishing boric acid from borate at the mineral surface. This is reasonably straightforward, as there is ample infrared spectral data for minerals containing trigonal (BO_3^{3-} and $B(OH)_3$) and tetrahedral B (BO_4^{5-} and $B(OH)_4^-$) boron groups (Ross, 1974). From the variation of mineral spectra with structure, it is possible to get a good grasp of what vibrational bands are accessible in the midinfrared region and how to interpret them. As one can see from Figure 1, some of these regions of infrared absorbance overlap. This fact makes conclusive peak assignment in samples with mixtures of trigonal and tetrahedral boron quite problematic. This is especially difficult when attempting to assign peaks for tetrahedral boron, as peaks from B-O-H bending, trigonal B-O stretching, and tetrahedral B-O stretching all occur in the 700–1000 cm^{-1} region.

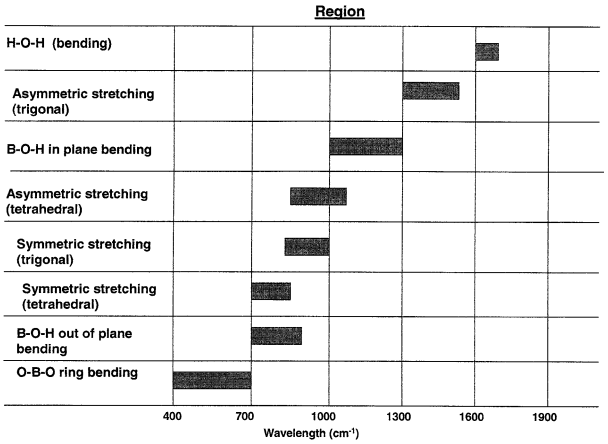

Fig. 1. Summary of infrared peaks of boric acid and borate that are accessible to in situ infrared studies. Adapted from Ross (1974).

None of the previous boron/mineral adsorption studies thoroughly discuss the relationship between infrared spectra and the structure of boric acid on the surface of minerals. This is likely due to the fact that the relationship between molecular symmetry and infrared spectra of boron containing compounds has not been specifically discussed in the infrared literature, as is the case for phosphate and sulfate (Nakamoto, 1986). This means that the symmetry rules must be worked out for the bands that are accessible for midinfrared spectroscopic studies in aqueous suspensions. Experimental constraints mean that the region from 800 to 1600 cm^{-1} is available for study. It is convenient to consider the O-H ligand as a single entity for purpose of determining symmetry rules. This is reasonable since the center of mass for B-O-H is not greatly shifted from the position of B-O molecules. One complication occurs with boric acid, since the hydroxyls are not symmetrical in crystal form and instead the protons are at an angle resulting in a horizontal axis of rotation. However, in aqueous solution, the movement of H around the O atom of boric acid is essentially unconstrained. Considering the OH of boric acid and borate as one entity results in molecules defined as YX3 and YX4 by Nakamoto (1986).

The relationship between molecular configuration and infrared spectra for boric acid and borate can be clearly defined using the symmetry rules for YX3 and YX4 molecules that were derived and explained in Nakamoto (1986). For free boric acid, the trigonal planar (YX3) molecule has D_{3h} symmetry,

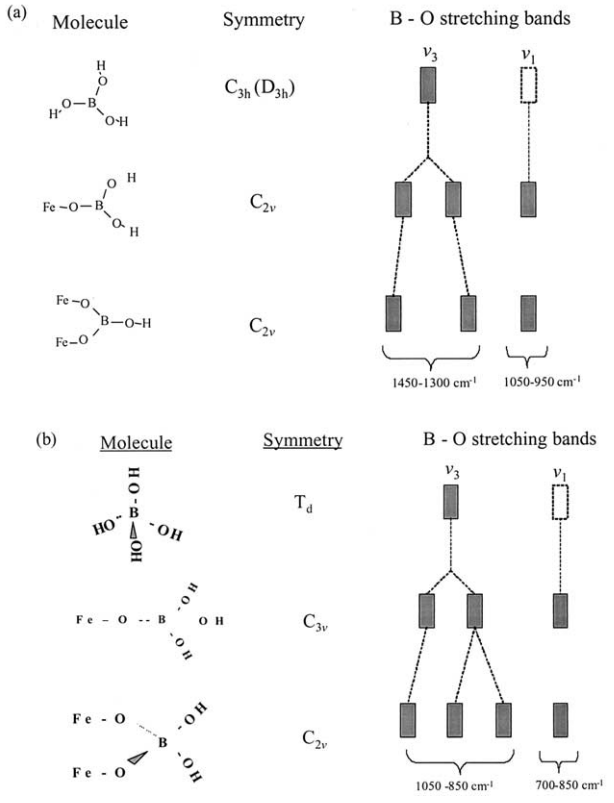

Fig. 2. Relationship between molecular symmetry and B-O vibrations of potentially occurring (a) boric acid and (b) borate surface complexes with HFO. In the case of aqueous boric acid, C_{3h} is the true symmetry, but OH was treated as a single entity so that D_{3h} symmetry could be used as an approximation.

and should have one IR active peak (1500–1300 cm^{-1}) for the asymmetric B-O stretching (ν_3) as well as an inactive or weakly IR active (depending upon the molecules distortion) symmetric B-O stretching (ν_1) band (1100–950 cm$_{-1}$). In pressed disks of solid boric acid, this ν_1 peak is clearly visible, but in aqueous solution it is not usually observed. If one proton of the boric acid molecule is substituted with metals (in our study Fe) then the symmetry of the molecule is lowered to C_{2v}. This reduction in symmetry causes the doubly degenerate asymmetric ν_3 band to lower in symmetry, and two peaks should be seen in the infrared spectrum between 1250 and 1500 cm^{-1}. The symmetric stretch also becomes fully infrared-active so there are a total of three B-O vibrations visible in a monodentate metal-boric acid complex. For bidentate metal boric acid complexation, the symmetry remains C_{2v}, and so the number of peaks remains unchanged. The splitting of the two ν_3 bands is expected to increase and/or shift when the number of iron atoms increases, but that is not sufficient to distinguish monodentate from bidentate boric acid. Nonetheless, infrared spectroscopy is capable of separating aqueous and inner-sphere boric acid from one another. The predicted changes in the infrared spectra of boric acid complexes with different symmetry are summarized in Figure 2a.

The symmetry of the tetrahedral borate molecule is identical to other YX4 molecules such as sulfate and phosphate, which have been extensively studied with infrared spectroscopy (Nakamoto, 1986). As the free borate anion, the molecule has T_d symmetry and one broad ν_3 asymmetric stretching band at approximately 950 cm^{-1}. The symmetric stretching (ν_1) band will be either weakly active or completely inactive, but it typically is obscured by water in any case. The symmetry of borate is lowered to C_{3v} by forming a monodentate complex with a single Fe atom and the ν_3 band splits into two peaks. If a bidentate complex is formed with two of the protons on borate being substituted by Fe, then the resulting complex has C_{2v} symmetry, the ν_3 band becomes fully degenerate, and three peaks will appear in the infrared spectrum. The predicted changes in the infrared spectra of borate complexes with different symmetry are summarized in Figure 2b.

The above discussion has separated the contributions of B-O-H bending modes to the overall spectra of boron compounds. However, in the actual spectra there are additional broad peaks that arise from in plane B-O-H bending (1300–1000 cm^{-1}) and out of plane bending (850–700 cm^{-1}). These vibrations overlap with some of the other B-O stretching vibrations and can make data analysis more difficult.

2. MATERIALS AND METHODS

All chemicals used in these experiments were reagent grade or better, and deionized distilled water (18 MΩ) was used for all studies.

2.1. Mineral Synthesis

The hydrous ferric oxide (HFO) used in all experiments was synthesized following the procedure in Schwertmann and Cornell (1991). A 500 mL solution of 1 M $Fe(NO_3)_3$ was prepared and placed into a 2L container. A lid was placed on the container with ports for a N_2 purge line, a mechanical overhead stirrer, a pH meter, a dispensing tip for a pH stat, and a sampling port with lid. The solution was stirred at ~300 rpm with the overhead stirrer and purged with nitrogen for approximately an hour, then a funnel was placed into the sampling port. Enough 1 M KOH was slowly poured into the container to raise the pH to a value of 5, and then the pH stat (Metrohm model 716) was engaged to dispense 1 M KOH to an end point of pH 7.5. The end point of pH 7.5 was maintained for 1 h, and then the iron hydroxide precipitate was separated into several 250mL high speed centrifuge bottles and washed via centrifugation (10000 rpm for 5 min) with 0.1 M NaCl. This washing procedure was repeated twice to remove any potassium and non-precipitated iron. Then, the solid was washed three more times using the same procedure with deionized H_2O and then placed into dialysis tubing and dialyzed in distilled water for 48 h. After dialysis, the solid was placed into a 1L container; the pH was lowered to 5.5 with 0.1 M HCl to minimize the amount of carbonate contamination, and stored at 5C until use in experiments. The solid density of this stock suspension was determined to be 18 g/L, and the surface area (N_2-BET) of the freeze-dried solid was 255 m^2/g. The PZC was determined to be 8.5 via potentiometric titrations in $NaClO_4$.

2.2. Sorption Experiments

All sorption experiments were done inside a glove box under N_2 atmosphere to eliminate CO_2 from the system. Initially, suspensions of HFO, background electrolyte (NaCl), and distilled-deionized H_2O (18 MΩ) were prepared with a final solid density of 1 g/L. The calculation for amount of background electrolyte added to obtain a final ionic strength of 0.01 mol/L was based upon the concentration of borate anion in the final sample as well as an estimation of the amount of acid or base needed to adjust the pH of the final sample. This suspension was adjusted to the desired pH and placed on a rotating shaker for ~ 8 h and then pH was measured and adjusted again. After 24 h, the suspensions were again adjusted to the proper pH, and boric acid was added from a 10 mM stock solution to the unreacted solids, and pH was again adjusted. At this time, a calculation was made to account for the

contribution of NaOH or HCl to the suspensions ionic strength and then to determine how much additional NaCl should be added to the suspension to obtain an ionic strength of 0.01 mol/L. The samples were then shaken for ~8 h and the pH was adjusted with either 0.01 M NaOH or 0.01 M HCl. The samples were adjusted for pH again at 24 h and 32 h while the reaction proceeded, and then after 48 h the pH was measured and the samples were filtered and the supernatent was acidified and analyzed via ICP-AES spectrometry.

2.3. ATR-FTIR Spectroscopy

A Perkin Elmer 1720X FTIR spectrometer was used for all spectroscopic studies. The instrument was equipped with a Whatman purge gas generator to remove water vapor and CO_2, a $N_{2(l)}$-cooled MCT detector, and a horizontal ATR-FTIR accessory from Spectra-Tech. Aqueous samples were placed in a trough sampler with a 45° ZnSe crystal, and adsorption studies were conducted using a Spectra Tech ATR-flow cell with a 45° ZnSe crystal. A more detailed explanation of the deposition method can be found in previous papers (Hug and Sulzberger, 1994; Hug, 1997; Peak et al., 1999, 2001; Wijnja and Schulthess, 2000; Elzinga et al., 2001). The primary advantage of the deposition technique is that it results in an extremely high solid concentration at the ZnSe crystal surface. Since adsorbate also accumulates at the mineral/water interface, the concentration of surface species in the path of the infrared beam is much higher than when applying pastes or slurries of mineral sorption samples. As a result, bulk solution concentrations of reactant can remain well below infrared detection limits while adsorption reactions proceed. The spectra collected are therefore only surface complexes of reactant, and typically have sharper and more easily resolved peaks than other ATR-FTIR techniques. All infrared spectra were analyzed using Peaksolve (Galactic Industries) by fitting a linear baseline through the data and then normalizing the spectra so that absorbance was equal to zero at 800 and 1800 cm^{-1}.

For the flow cell experiments, a small quantity (~3mg) of HFO was deposited on the surface of the ZnSe crystal and allowed to air dry. Then, the deposit was carefully washed several times with background electrolyte to remove any non-adhering HFO, allowed to dry again, and placed into the flow cell. The flow cell was then placed into the FTIR, and Tygon tubing was used to connect the flow cell to a peristaltic pump and reaction vessel. The reaction vessel was nitrogen purged, well mixed with a stir bar, and pH was monitored with a Corning pH electrode. Additions of 0.01 M acid or base were made with Rainen electronic pipette to adjust pH to the desired value. Initially, a background electrolyte of 0.01 M NaCl was pumped through the flow cell at a rate of 1.0 mL min^{-1}. An infrared spectrum of the entire flow cell assembly (background electrolyte solution, HFO, and ZnSe crystal) was collected as a reference and then subtracted from spectra collected at later times to monitor changes in the infrared spectra. Initially, the spectra will change as a function of time due to carbonate desorption, protonation or deprotonation of the HFO surface hydroxyls, rehydration of the HFO, changes in ionic strength, and removal of a small amount of HFO from the system via the flow of background electrolyte. After approximately 2 h, no further change in the spectra was observed, and so a new background was collected to be used for all successive scans. At this time boric acid was added at a known amount, allowed to react with the HFO surface, and adsorption spectra were collected. Equilibrium was operationally defined in all experiments as being reached when spectra collected 15 min apart showed no change in absorbance intensity. Each addition required from 30 min to 2 h to come to operationally-defined equilibrium with the surface, and required reaction time was found to be inversely related to boric acid concentration in solution. After collecting a spectrum of boric acid at a given solution concentration, more boric acid was then added to the reaction vessel and the process was repeated to generate adsorption isotherms inside the flow cell.

3. RESULTS AND DISCUSSION

Results from adsorption isotherms conducted at pH 6.5, 9.4, and 10.4 are shown in Figure 3. In all cases, samples were prepared volumetrically and an ionic strength of 0.01 M NaCl and a 0.5 gL^{-1} solid density were used. No attempts were made to convert the surface loading from μmoles per gram to μmoles per m^2, as the surface area for a freeze-dried HFO is undoubtedly quite different from that of a freshly prepared HFO gel. From the isotherm there are several aspects of boron adsorption of interest. First of all, boron sorption is close to a maximum at pH 9.4, which is the pK of boric acid. Boron adsorption decreases rapidly above the pK of boric acid. Additionally, the isotherms do not display a particularly high affinity of boric acid for the HFO surface: to achieve a high surface loading, a high solution concentration must also be present. In fact, all isotherms exhibit an "S-shaped" curve, which suggests that at low concentrations boron has a low affinity for the surface, with an increasing affinity for adsorption as equilibrium solution concentrations increase. This type of isotherm was explained by Sposito (1989) as being due to competition between the solution phase and the solid surface for the adsorbate. For organic compounds, it was proposed that solution polymerization might be occurring, and that the resulting polymers have a higher affinity for the surface. In the isotherms in Figure 4, this would suggest a concentration around 750 μM where polymerization would begin to occur. There are some problems with this explanation, however. First of all, 750 μM is far below the solution polymerization value for boric acid. Second, the S-shaped isotherms occur at pH 6.5 although polymerization is not predicted to occur in solution at this pH. Alternatively, You and coworkers (2002) have suggested that S-shaped isotherms might occur due to hydrophobicity of the adsorptive. As adsorption of hydrophobic molecules occur, the sorbent phase changes from hydrophilic to hydrophobic. At low concentrations, adsorption is limited by the hydrophilicity of the sorbent, and at higher concentrations, adsorption is enhanced by hydrophobic interactions between hydrophobic molecules on the surface. FTIR studies were conducted at concentrations between 50 μM and 1 mM to limit the importance of any potentially occurring polymerization. Spectra at 1 mM were compared to those taken at lower concentration, but no significant change in peak intensity or position could be determined.

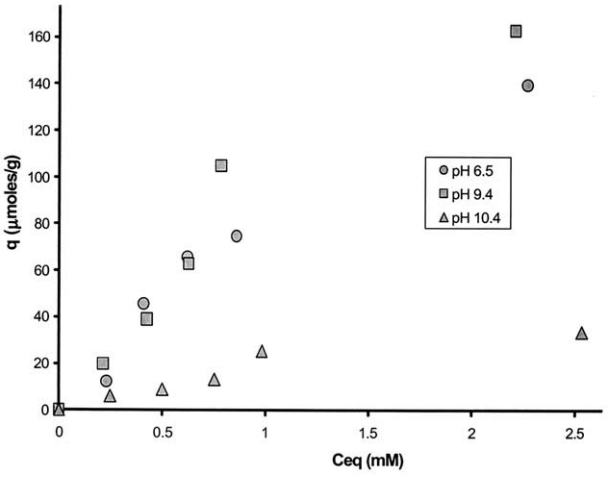

Fig. 3. Boron on HFO adsorption isotherms at three different pH values. For all experiments, an ionic strength of 0.01 M (NaCl) and a suspension density of 0.5 g/L was used. Note the S-shaped isotherm.

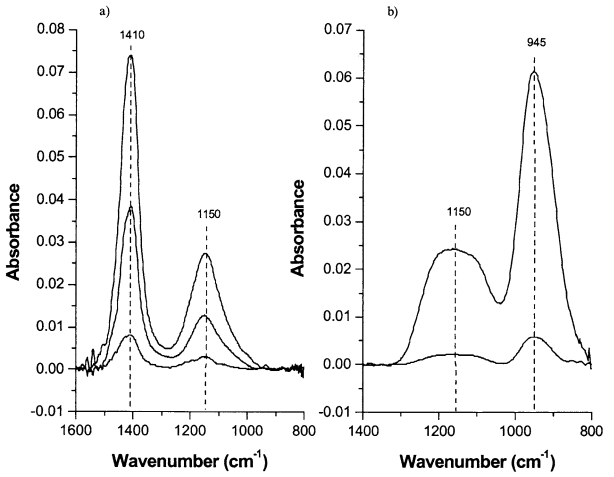

Fig. 4. ATR-FTIR spectra of (a) boric acid and (b) borate collected at different concentrations. For boric acid in (a), concentrations (from bottom) were 10, 50, and 100 mM total boron. For (b), total boron concentrations are (from bottom) 10, and 100 mM.

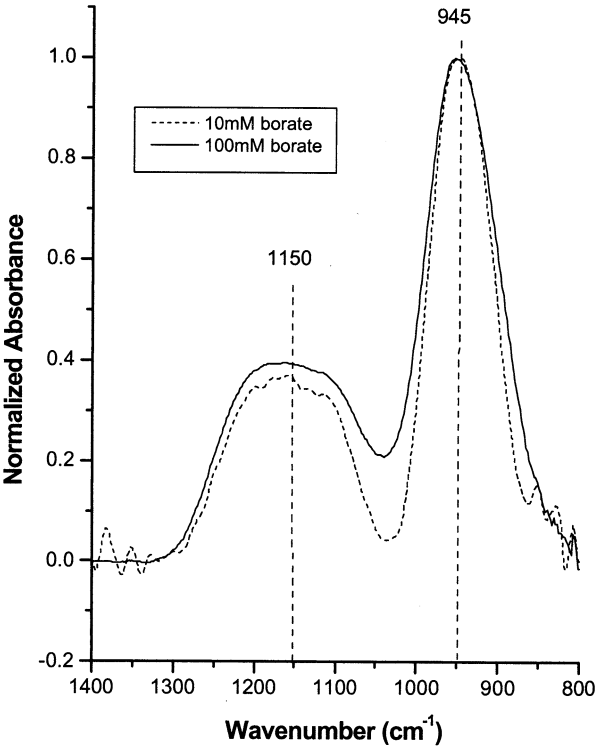

Fig. 5. Borate spectra from Figure 4b that were normalized to a maximum absorbance of 1.0. The solid line is 100 mM borate, and the dashed line is 10 mM borate. Note the broadening of the B-O peak at 945 cm^{-1} in the 100 mM spectrum; peak width at half height is 72.4 $\pm$ 0.8 for 10 mM borate and 89.6 $\pm$ 0.7 for 100 mM borate.

There is no clear sorption maximum for any of the isotherms, which could be due to the high surface area of the HFO studied, or it might be due to polymerization reactions on the surface.

While adsorption experiments were all conducted far below aqueous polymerization levels, aqueous boric acid and borate spectra were collected for concentrations both below and above polymerization thresholds. This was done to examine the effects of polymerization on the aqueous boric acid and borate spectra. Figure 4 shows the spectra of boric acid at pH 6.5 (Fig. 4a) and at pH 11.5 as its conjugate base borate (Fig. 4b). For the trigonal planar boric acid, one can clearly see one peak at 1400 cm^{-1} caused by asymmetric B-O stretching (v_3) as well as the in-plane B-O-H bending at 1150 cm^{-1}. For borate, the asymmetric stretching band occurs at 950 cm^{-1}, while the B-O-H in plane bending appears in a similar location to the trigonal species ($\sim$ 1150 cm^{-1}). The in-plane bending peak of borate is much broader than boric acid, suggesting that there is a range in molecular configuration, and possibly more than one peak in the region. This effect is fairly pronounced at 100 mM, which is consistent with the observation (Cotton and Wilkinson, 1985) that boric acid polymerizes in aqueous solution at concentrations above 25 mM and above pH 7. The presence of some tetrahedral boron polymers would result in both multiple OH vibrations (as observed) and splitting of the v_3 band at 950 cm-l due to lowered symmetry of coordinated borate. However, we were unable to observe separation of the 950 cm^{-1} peak into multiple peaks at 100 mM borate. This is likely due to the overwhelming concentration of aqueous borate monomers in the 100 mM sample that masks the spectral features of the polymerized forms. When spectra are normalized to the same maximum absorbance (Fig. 5) there are slight differences that can be observed. At 100 mM, there is some broadening of the B-O peak that could represent the presence of some polymeric borate. Peak fitting of the normalized and background subtracted spectra (with gaussian peaks) resulted in a peak width at half height of 72.4 $\pm$ 0.8 at 10 mM borate and 89.6 $\pm$ 0.7 at 100 mM borate. This might be due to the appearance of additional peaks that are masked by the broad aqueous borate spectrum, or it may indicate that splitting of the v_3 band is simply very weak for borate. In any case, it is very difficult to determine bonding mechanisms of borate from FTIR spectra without clear separation of the v_3 band into multiple peaks. Aqueous monomeric, polymers, outer-sphere, and inner-sphere borate may therefore have somewhat similar midinfrared spectra and be difficult to distinguish from one another. In adsorption experiments, solution borate concentrations will always be below detection limits, so that contribution to the spectra can be eliminated. While not directly measured by spectroscopy, it may be possible to further distinguish outer-sphere from inner-sphere borate by conducting adsorption studies over a range of pH. Above the point of zero charge of HFO ($\sim$8–9), the surface is negatively charged and therefore unlikely to adsorb borate as an outer-sphere complex.

Infrared spectra from an adsorption isotherm of boric acid on HFO at pH 6.5 and I = 0.01 M are shown in Figure 6. Figure 6a shows the full spectra from 1800–800 cm^{-1}, while Figure 6b shows only the 1100 to 800 cm^{-1} region in more detail. There are several features that are common to all of the adsorption spectra that were collected, so they should be discussed first. All of the spectra feature negative absorbance peaks at 1625 cm^{-1} and at 1490 cm^{-1}. These peaks are from the loss of water and carbonate (respectively) from the HFO surface. In the case of carbonate, it is quite likely that there is some strongly bound carbonate present at the HFO surface (from being exposed to air while drying) that is not being

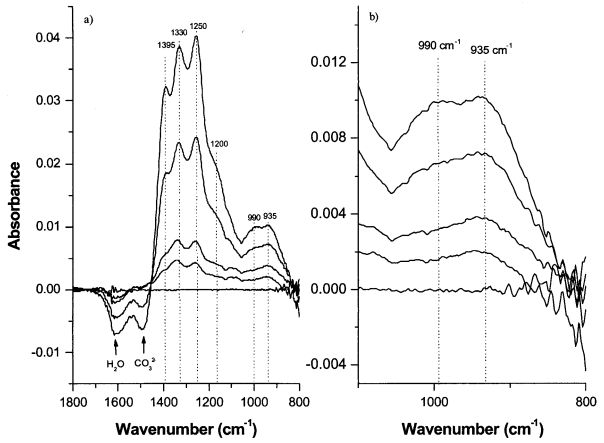

Fig. 6. ATR-FTIR spectra of boron adsorbed on the HFO surface at pH 6.5 and I = 0.01 M as a function of concentration. Aqueous equilibrium boron concentrations are (from bottom) 0, 50, 100, 500, and 1000 μM. (b) Same samples as in (a) with the 1100–800 cm^{-1} region expanded for clarity.

desorbed as the system equilibrates. This carbonate could possibly be desorbed as the adsorption of boric acid occurs.

The remaining peaks in the spectra are the result of adsorbed boric acid on the HFO surface. There are three peaks in the region of trigonal B-O v_3 bands, at 1395, 1330, and 1250 cm^{-1}. Since the v_3 band of trigonal boron complexes is only doubly degenerate, there must be more than one surface species present to account for three distinct peaks in this region. There are two possibilities that could result in multiple surface complexes. It is possible that the peak at 1250 cm^{-1} (which is larger in intensity than the other peaks) is present in the same position for both monodentate and bidentate trigonal boron while the other two peaks represent a monodentate and a bidentate bonding environment. This seems rather unlikely. Another possibility is that the peak at 1395 cm^{-1} is a separate trigonal species with symmetry similar to aqueous boric acid, while the second complex with peaks at 1330 and 1250 cm^{-1} is the result of an inner-sphere trigonal surface complex. Several common boric acid species are potential sources of the 1395 cm^{-1} peak: aqueous boric acid, polymeric trigonal boron, and outer-sphere boric acid. Two of the possibilities can be eliminated: the solution concentrations are below detection limit for aqueous boric acid, and at pH 6.5 boron does not polymerize. Therefore, this D_{3h} symmetry surface complex is best explained by outer-sphere complexation of boric acid to the HFO surface.

The observation that a neutral molecule (boric acid) can adsorb as an outer-sphere surface complex on the iron oxide surface at first seems counter-intuitive, as outer-sphere complexation typically occurs due to electrostatic attraction of an ion for an oppositely charged surface. However, if one considers that boric acid is a Lewis acid (electron pair acceptor), then attraction to the surface becomes more reasonable. The Lewis acid boron metal center will have an affinity for the Lewis base oxygen of a surface functional group, and will be attracted to electron density of the O atoms of the many surface hydroxyls and bound waters at the HFO/aqueous interface. This Lewis acid/base pairing may be further stabilized by hydrogen bonding. Outer-sphere surface complexes of the neutral $As(OH)_3$ molecule have been observed to form on iron and aluminum oxides using Raman spectroscopy (Goldberg and Johnston, 2001) and on aluminum hydroxides using EXAFS spectroscopy (Arai et al., 2001) at pH below the PZC of the metal oxide.

As pH will affect surface charge, boric acid speciation, and functional group speciation, it will be useful to monitor changes in the intensity and position of the peak at 1395 cm^{-1} as pH changes. The B-O-H in-plane bending is present in the adsorption spectra as predicted from theory, but shifted to somewhat higher wavenumber (1200 cm^{-1} vs. 1150 cm^{-1} for aqueous boric acid). The overlapping peaks due to the trigonal B-O vibrations make it impossible to draw much information from the OH bending as the peaks are mostly obscured.

Figure 6b expands the spectra from Figure 6a so that bands in the 1100 to 800 cm-1 region can be more clearly discerned. There are at least two overlapping peaks in this region observed at 990 and 935 cm^{-1}. The first instinct would be to assume that these arise from the v_3 asymmetric stretch of tetrahedral borate, and that the borate adsorbs on the surface as a monodentate complex with C_{3v} symmetry. Accordingly, the peak at 985 cm^{-1} was previously (Su and Suarez, 1995) attributed to tetrahedral borate adsorption in the literature. However, when boric acid forms inner sphere complexes (as observed by the strong splitting of the trigonal v_3 peaks in Fig. 6a) then the symmetric stretching band (v_1) should also become infrared-active in the 1100–950 cm^{-1} range. Based upon the spectra at pH 9.4 and 10.4 (to be discussed later), the peak at 1005 cm^{-1} can be assigned to the v_1 from inner-sphere boric acid surface complexation. The remaining peak at 940 cm^{-1} is either a result of borate on the surface or is due to vibrations from out of plane B-O-H bending. The broadness of the peak (PWHH of 146cm^{-1}) indicates that multiple peaks may be present and overlap to generate a single broad peak. It would be convenient to assign the single broad peak to outer-sphere borate adsorption, but at pH 6.5 solution borate concentrations are extremely small (~0.1%) and it is unlikely that outer-sphere borate accumulation at the surface would occur.

Figure 7 shows the spectra of boric acid adsorbed on the HFO surface at 9.4, which is close to the pK of boric acid as well as slightly above the PZC of HFO. The most obvious differences between the spectra at pH 6.5 and pH 9.4 are the disappearance of the peak at 1395 cm^{-1} and the increase in the absorbance in the 800–1000 cm^{-1} region when pH is raised to 9.4. The disappearance of the 1395 cm^{-1} peak (attributed to physically adsorbed boric acid) is consistent the observation that outer-sphere complexation of arsenite vanishes above the PZC of the sorbent. The remaining trigonal v_3 peaks at 1250 and 1330 cm^{-1} are again consistent with inner-sphere boric acid adsorption. In Figure 7b, the region where tetrahedral boron bands are expected is shown in greater detail. As with Figure 6b, there are two infrared-active peaks at 995 and 935 cm^{-1}. The peak at 935 cm^{-1} has a greater intensity at pH 9.4 than it does at pH 6.5, which is consistent with the assignment of the 935 cm^{-1} peak to tetrahedral B-O v_3. At pH 9.5the borate concentrations in solution are approximately 50% of the total boron concentration at pH 9.4 and so more borate is expected at the surface than at pH 6.5 when only ~0.1% is tetrahedral in solution. When the results of peak fitting are compared, the area under the peaks at ~1000 vs. ~940 cm^{-1}

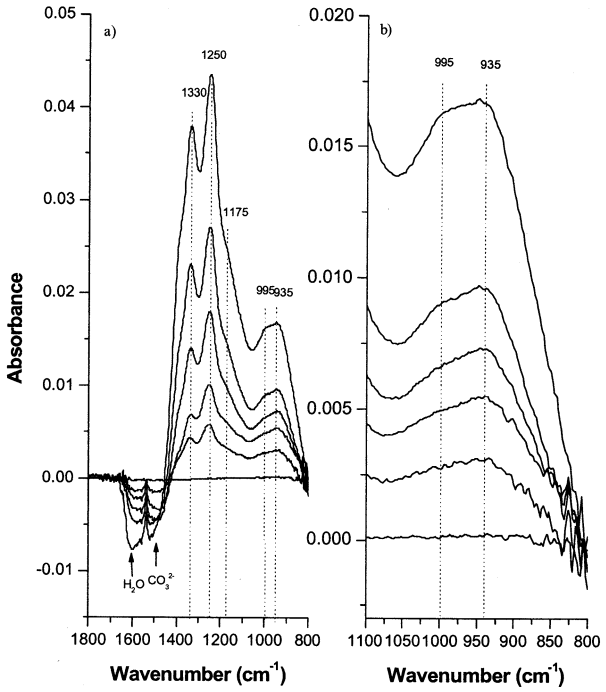

Fig. 7. ATR-FTIR spectra of boron adsorbed on the HFO surface at pH 9.4 and I = 0.01 M as a function of concentration. Aqueous equilibrium boron .concentrations are (from bottom) 0, 50, 100, 250, 500, and 1000 μM. (b) Same samples as in (a) with the 1100–800 cm^{-1} region expanded for clarity.

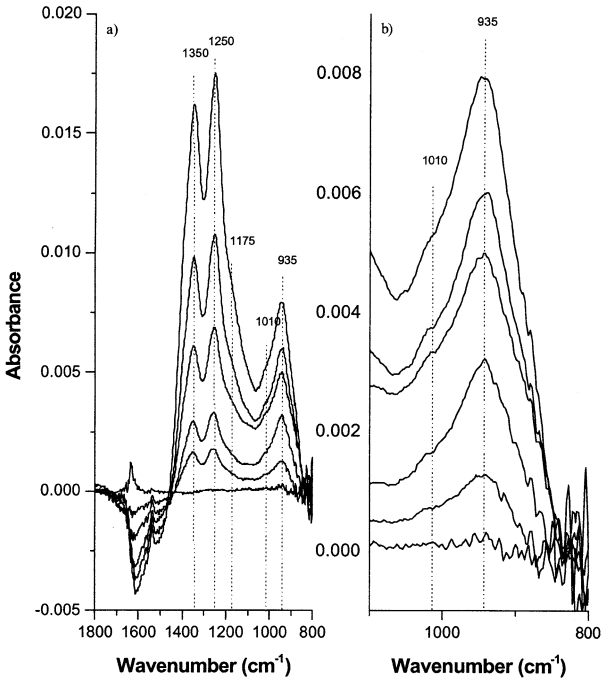

Fig. 8. ATR-FTIR spectra of boron adsorbed on the HFO surface at pH 10.4 and I = 0.01 M as a function of concentration. Aqueous equilibrium boron concentrations are (from bottom) 0, 50, 100, 250, 500, and 1000 μM. (b) Same samples as in (a) with the 1100–800 cm^{-1} region expanded for clarity.

changes from 0.73:1 at pH 6.5 to 0.68:1 at pH 9.4. Background subtraction becomes difficult due to water interferences in this region, so there is some difficulty in determining the absolute importance of the peak at 935 cm^{-1} to the absorbance in the 800–1100 cm^{-1} range.

Finally, the spectra of boric acid adsorbed on HFO at pH 10.4 are shown in Figure 8. The spectra all appear very similar to the pH 9.4 data with two exceptions: (1) the overall absorbance is less at 10.4 than at pH 9.4 (indicating that less boric acid is adsorbed on the HFO surface) and (2) more of the total absorbance occurs in the 1000–800 cm^{-1} region at pH 10.4. One can still see two clear asymmetric stretching peaks between 1250 and 1350 as well as the shoulder at 1010 cm^{-1} that is diagnostic for inner-sphere boric acid adsorption. It is noteworthy that the ν_1 band shifted almost 10 cm^{-1} when pH is adjusted from 9.4 to 10.4. Studies of boric acid-containing minerals and polymers typically report values of around 1075–950 cm^{-1} (Ross, 1974) for the ν_1 band, so this peak still falls within the predicted range. A shift in position could be caused by a conformational change of boric acid from monodentate to bidentate at the HFO surface, or it alternatively could be caused by a new trigonal species (such as multinuclear boron clusters with some boric acid moieties). The peak at observed as a relatively strong shoulder at 1000 cm^{-1} in the pH 6.5 data is now much weaker than the peak at 935 cm^{-1}. The ratio of peak areas for the fitted peaks at 1000 vs. 940 cm^{-1} produces a ratio of 0.73:1 at pH 6.5, and at pH 10.5 the ratio of areas is further reduced to 0.49:1. No clear splitting of the ν_3 band can be observed in the spectra, although the peak is very broad. There are two reasonable explanations for the inability to see distinctive splitting of tetrahedral ν_3 vibrational bands in the results. Potentially, there could be a multitude of different borate inner-sphere surface complexes that overlap and produce a single broad band. Alternatively, it was observed in the pH 11.5 solution spectra of Figure 5 that even in the presence of borate polymers that little splitting of the ν_3 bands occurs. It is possible that polymeric boron of a tetrahedral (or mixed tetrahedral and trigonal) geometry could result in the broad single peak at 935 cm^{-1}. However, the solution concentrations were well below the established aqueous polymerization level of 25 mM (5–500 μM aqueous boric acid was used in the present studies). Previous researchers (Alvarez and Sparks, 1985) have shown with in situ spectroscopic techniques that silicate polymerization may occur at surprisingly low concentrations (~100 μM). The same might be possible for borate and so this possibility cannot completely be discounted.

Peak fitting is quite difficult for the obtained spectra due to the many peaks that are present as well as the difficulty of baseline subtraction at low wavenumber. Figure 9 shows the results of spectral peak fitting of the 500 μM boric acid spectra at pH 6.5 (Fig. 9a) and pH 10.5 (Fig. 9b). Lorentzian peaks were used to fit the data, and there are several items of note in the fits. The most interesting item for discussion is the 1100–800 cm-1 region of the data. There are two distinct peaks in this region: a peak attributed to the asymmetric stretch of adsorbed borate centered at 925 cm^{-1} at pH 6.5 and at 935 cm^{-1} at pH 10.5 and a second peak attributed to the symmetric stretch of adsorbed boric acid centered at 1005 cm^{-1} at pH 5.6 and at 1023 cm^{-1} at pH 10.5. The large shift in these peaks with

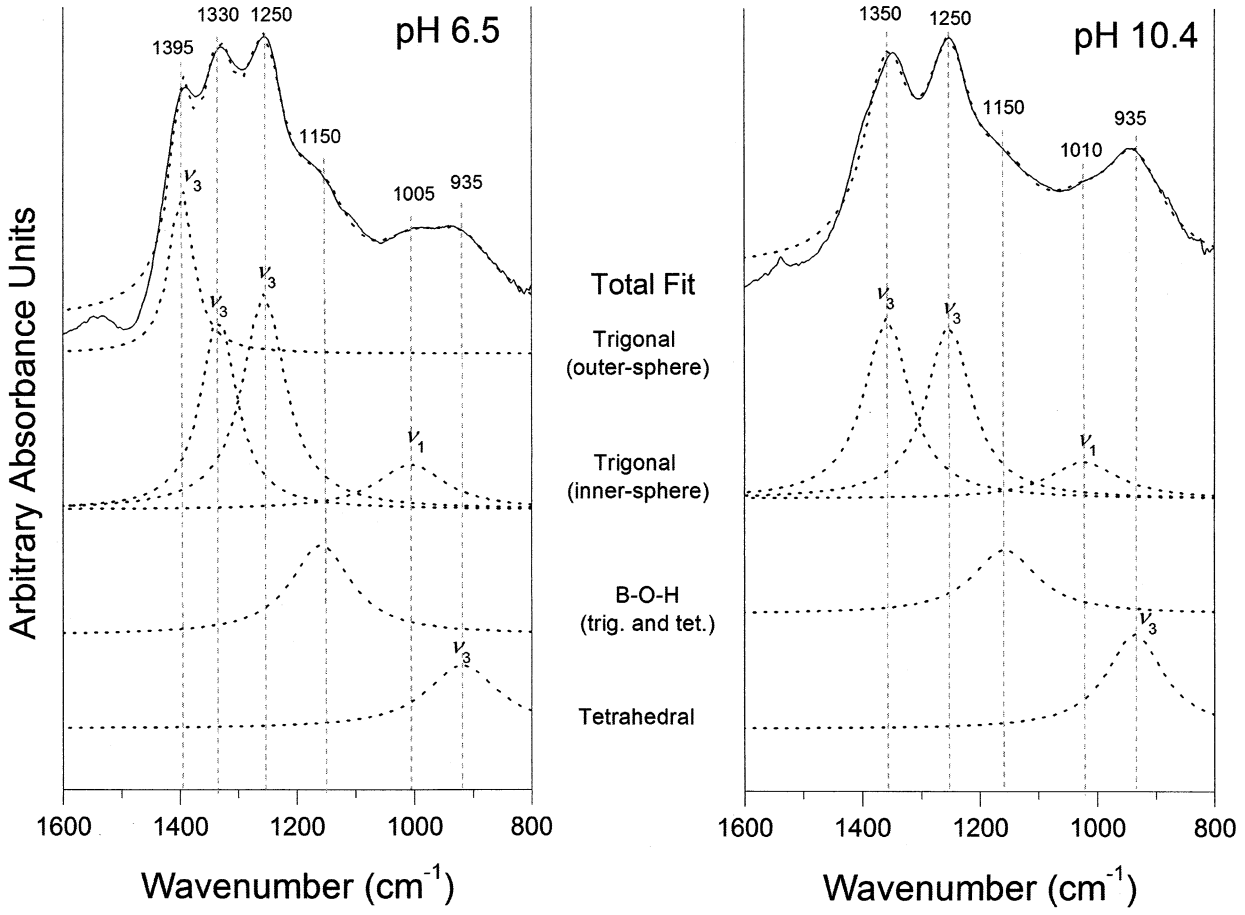

Fig. 9. Results of fitting Lorentzian peaks to boric acid adsorption data at pH 6.5 and pH 10.5. The total fit is shown with raw spectra overlain, and then the individual peaks are grouped due to their assignment in the discussion. At pH 10.5, note the disappearance of the peak at 1395 cm^{-1} and the increasing importance of the peak at 935 cm^{-1} to the overall absorbance between 1100 and 800 cm^{-1}.

changing pH, along with the broadness of the fitted peaks (the peak width at half heights are larger for these two peaks than from the trigonal peaks that are over twice as large), suggests that there are more peaks present that cannot be resolved by simple peak fitting routines. This strengthens the theory that there is inner-sphere borate present at the surface, and that the bands simply overlap too much to make exact identification possible with the present ATR-FTIR data.

Possible mechanisms consistent with the observed spectra for adsorbed boron are illustrated in Figure 10. It was not possible to distinguish monodentate from bidentate complexes with our FTIR results, so reaction mechanisms that explain conversion from monodentate to bidentate are proposed as possible.

Mechanisms in Figure 10a discuss reactions of trigonal boric acid with FeOH groups on the HFO surface to produce both trigonal and tetrahedral surface complexes. Initially, an outer-sphere surface complex is formed as a result of the Lewis acidity of the boron metal center. This surface complex is observed as a peak at 1395 cm^{-1} in the pH 6.5 adsorption spectra. Since the peak persists even when operationally-defined equilibrium has been reached, it appears to be a stable surface species rather than a transient intermediate. Once outer-sphere surface complexation occurs, ligand exchange can proceed in two separate pathways that produce either trigonal or tetrahedral inner-sphere surface complexes of boron. For the trigonal complexes, a water ligand would be displaced. This can occur due to strengthening of the boron Lewis acid/base bond with the surface hydroxyl's oxygen accompanied by the weakening of the surface functional group's proton bond. This increases the stability of the hydrogen bonding between a boric acid hydroxyl and the surface hydroxyl's proton, producing a water ligand which is released. Since all of the molecules and surface groups involved in this reaction are formally neutral, there is no change in the surface charge (or overall pH) that would accompany these reactions. This reaction would be expected to occur more favorably at neutral to slightly alkaline pH values where both the FeOH surface group and boric acid are the dominant species.

Also in Figure 10a is a second pathway following outer-sphere boric acid adsorption. Instead of a ligand-exchange reaction accompanied with release of water, a proton from the surface hydroxyl is the leaving ligand. This causes a shift in conformation to tetrahedral boron on the HFO surface. Forma-

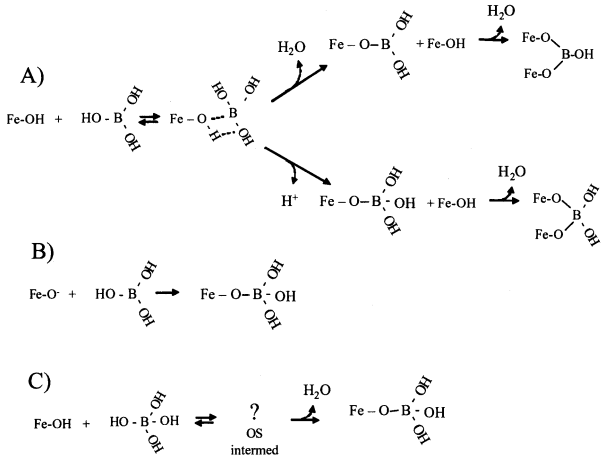

Fig. 10. Possible reactions mechanisms of boric acid at the HFO surface. ATR-FTIR spectroscopy suggest that the most likely mechanisms are the ones in pathway (a).

tion of tetrahedral boron on the surface from a trigonal outer-sphere intermediate is consistent with the observation of tetrahedral boron at the surface at pH 6.5 since borate in solution is not necessary for this reaction pathway to occur. The observation that borate adsorption becomes more pronounced at higher pH is also consistent with this mechanism since H^+ released into solution via ligand exchange will rapidly be neutralized (thus driving the reaction). The release of a proton from the surface in the ligand exchange reaction would also result in surface charge becoming more negative, which is consistent with previous electrophoretic mobility measurements (Suarez et al., 1988). This mechanism is also consistent the important observation of macroscopic experiments that boron adsorption decreases markedly above the pK of boric acid since concentrations of boric acid would greatly affect reactivity in 10a.

Figure 10b demonstrates a second potential reaction mechanism: direct formation of an inner-sphere surface complex via a Lewis acid-base mechanism. This mechanism is not likely to be particularly important. For FeO^- to be present, the solution pH must be very high (typically several units above the PZC). Conversion of boric acid to borate in solution will also occur at high pH, so the concentrations of the reactants for 10b are not expected to ever simultaneously be present in large quantities.

Finally, Figure 10c discusses potential mechanisms of borate adsorption. For an inner-sphere complex to form between a surface hydroxyl and borate, an outer-sphere intermediate would typically be needed to bring the borate to the surface. There was no evidence of any such intermediate, though the extremely broad borate v_3 bands might contain a peak arising from outer-sphere borate. This outer-sphere complex would have to be dominated by hydrogen-bonding since the surface is either neutral or negatively-charged at pH where borate forms in solution. Alternatively, a 5-coordinate boron intermediate would be needed (though this is not probable for boron). This complex would then undergo ligand exchange to form an inner-sphere borate surface complex. Because there is no clear driving force for the initial intermediate, this set of reaction mechanisms also seems less reasonable than 10a.

4. CONCLUSIONS

The chemistry of boron adsorption is both varied and complex, with multiple surface inner-sphere surface complexes occurring (trigonal and tetrahedral) and with the additional formation of outer-sphere surface complexes of boric acid. The geometry of inner-sphere boron surface complexes (trigonal versus tetrahedral) is always quite different than the speciation of boron in the bulk solution. By approaching the adsorption reaction from a mechanistic standpoint, this anomaly can largely be explained by the reaction of boric acid to form an outer-sphere intermediate complex that reacts with the HFO functional groups to form trigonal or tetrahedral complexes. Borate is not required in solution for tetrahedral boron to be present at the surface, since ligand exchange reactions could result in a conversion of boric acid to tetrahedral geometry at the surface. As pH is increased, the amount of tetrahedral boron on the surface also increases due not primarily to changes in surface speciation of boron but instead due to an increased tendency for proton release (and formation of tetrahedral boron complexes) rather than water release (and maintaining trigonal geometry) in the ligand exchange reaction. Other reaction mechanisms seem less favorable, and so the dominant reactant is predicted to be boric acid.

Outer-sphere boric acid complexation is also substantial on HFO at pH 6.5. The presence of outer-sphere boron adsorption has some important implications for plant toxicity and availability. Since physically-bound boric acid can be readily leached, it can be expected to move with water flow in soils. This is consistent with high boron content in irrigation water in arid regions as well as consistent with low boron concentrations in humid regions where boron leaches from the surface soils. Outer-sphere boron would also be expected to be more available for plant uptake than more strongly bound boron complexes because it should more readily return to the soil solution when concentrations in the bulk decrease.

Some negative absorbance consistent with residual carbonate being desorbed from the HFO surface was observed upon boric acid adsorption. This suggests that boric acid and dissolved CO_2 species may be competing to some extent for the same surface sites on HFO. In natural systems, carbonate concentrations in solution and on surfaces are expected to be substantially higher than those of boric acid, and there is a need for research to investigate how the presence of dissolved CO_2 influences boric acid surface chemistry.

Acknowledgments—D. Peak wishes to thank the National Science Foundation for a graduate fellowship as well as research funding.

Associate editor: D. Vaughan

REFERENCES

Alvarez R. and Sparks D. L. (1985) Polymerization of silicate anions in solutions at low concentrations. *Nature* **318,** 649–651.

Arai Y., Elzinga E. J., and Sparks D. L. (2001) X-ray absorption spectroscopic investigation of arsenite and arsenite adsorption at the aluminum oxide-water interface. J. Colloid interf. Sci. 235, 80–88.

Beyrouty C. A., van Scoyoc G. E., and Feldkamp J. R. (1984) Evidence supporting specific adsorption of boron on synthetic aluminum hydroxides. *Soil Sci. Soc. Am. J.* **48,** 284–287.

Cotton F. A. and Wilkinson G. (1980) *Advanced Inorganic Chemistry*. New York, Wiley.

Elzinga E. J., Peak D., and Sparks D. L. (2001) Spectroscopic studies of Pb(II)-sulfate interactions at the goethite–water interface. *Geochim. Cosmochim. Acta* **65,** 2219–2230.

Goldberg S., Forster H. S., and Heick E. L. (1993) Boron adsorption mechanisms on oxides, clay minerals, and soils inferred from ionic strength effects. *Soil Sci. Soc. Am. J.* **57,** 704–708.

Goldberg S. and Johnston C. T. (2001) Mechanisms of arsenic adsorption on amorphous oxides evaluated using macroscopic measurements, vibrational spectroscopy, and surface complexation modeling. *J. Colloid Interface Sci.* **234,** 204–216.

Hug S. J. (1997) *In situ* Fourier transform infrared measurements of sulfate adsorption on hematite in aqueous solutions. *J. Colloid Interface Sci.* **188,** 415–422.

Hug S. J. and Sulzberger B. (1994) *In situ* Fourier transform infrared spectroscopic evidence for the formation of several different surface complexes of oxalate on TiO_2 in the aqueous phase. *Langmuir* **10**(10), 3587–3597.

Keren R. and O'Conner G. A. (1982) Effect of exchangeable ions and ionic strength on boron adsorption by montmorillonite and illite. *Clays Clay Miner.* **30,** 341–346.

Keren R. and Bigham F. T. (1985) Boron in water, soils, and plants. In *Advances in Soil Science*. (Stewart B. E., ed) Springer-Verlag. 229–276.

Keren R. and Sparks D. L. (1994) Effect of pH and ionic strength on boron adsorption by pyrophyllite. *Soil Sci. Soc. Am. J.* **58,** 1095–1100.

McBride M. B. (1997) A critique of diffuse double layer models applied to colloid and surface chemistry. Clays Clay Miner. 45(4), 598–608.

Nakamoto K. (1986) *Infrared and Raman Spectra of Inorganic and Coordination Compounds*. Wiley.

Peak D., Elzinga E. J., and Sparks D. L. (2001) Understanding sulfate adsorption mechanisms on iron (III) oxides and hydroxides: results from ATR-FTIR spectroscopy. In Heavy Metals Release in soils (Selim H. M. and Sparks D. L., eds). Lewis Publishers, Boca Raton, pp. 167–190.

Peak D., Ford R. G., and Sparks D. L. (1999) An *in situ* ATR-FTR investigation of sulfate bonding mechanisms on goethite. *J. Colloid Interface Sci.* **218,** 289–299.

Ross S. D. (1974) Borates. *The Infrared Spectra of Minerals* In (ed. V. C. Farmer). Mineralogical Society, London. 205–226.

Schwertmann U. and Cornell R. M. (1991) *Iron Oxides in the Laboratory: Preparation and Characterization*. Weinheim.

Shriver D. F., Atkins P., and Langford C. H. (1994) *Inorganic Chemistry*. W. H. Freeman.

Sposito G. S. (1989) *The Chemistry of Soils*. Oxford University Press.

Su C. and Suarez D. L. (1995) Coordination of adsorbed boron: A FTIR spectroscopic study. *Environ. Sci. Technol.* **29,** 302–311.

Su C. and Suarez D. L. (1997) Boron sorption and release by allophane. *Soil Sci. Soc. Am. J.* **61,** 69–77.

Suarez D. L., Goldberg S., and Su C. (1998) Evaluation of oxyanion adsorption mechanisms on oxides using FTIR spectroscopy and electrophoretic mobility. In *Mineral–Water Interfacial Reactions: Kinetics and Mechanisms* (eds. D. L. Sparks and T. J. Grundl). ACS Symposium Series 715, Chapter 8, p. 136–178.

Wijnja H. and Schulthess C. P. (2000) Vibrational spectroscopy study of selenate and sulfate adsorption mechanisms on Fe and Al (hydr)oxide surfaces. *J. Colloid Interface Sci.* **229,** 286–297.

You Y., Zhao H., and Vance G. F. (2002) Adsorption of dicamba (3,6-dichloro-2-methoxy benzoic acid) in aqueous solution by calcined-layered double hydroxide. *Appl. Clay Sci.* **21,** 217–226.